Aeolian Research 21 (2016) 53–60

Contents lists available at ScienceDirect

Aeolian Research

journal homepage: www.elsevier.com/locate/aeolia

Aeolian sediment transport over gobi: Field studies atop the Mogao Grottoes, China

Lihai Tan, Weimin Zhang *, Jianjun Qu, Junzhan Wang, Zhishan An, Fang Li

Dunhuang Gobi Desert Research Station, Cold and Arid Regions Environmental and Engineering Research Institute, CAS, China

ARTICLE INFO

Article history:
Received 25 November 2015
Revised 4 March 2016
Accepted 4 March 2016

Keywords:
Gobi
Aeolian sediment transport
Entrainment threshold
Saltation

ABSTRACT

This paper reports on field studies of aeolian sediment transport over a rough surface-gobi atop the Mogao Grottoes, China, in relation to sediment entrainment, saltation mass flux and transport rate prediction. Wind speeds were measured with five cup anemometers at different heights and sediment entrainment and transport measured with horizontal and vertical sediment traps coupled to weighing sensors, where sediment entrainment and transport were measured synchronously with wind speeds. Four sediment transport events, with a measurement duration ranging between 2.5 and 11 h, were studied. The entrainment threshold determined by the horizontal sediment trap varied between 0.28 and 0.33 m s^{-1}, and the effect of non-erodible roughness elements-gravels increased the entrainment threshold approximately by 1.8 times compared to a uniform sand surface. Unlike the non-monotone curve shape of sediment flux density profile over gobi measured in wind tunnels, the flux density profile measured in the field showed an exponential form. Aeolian sediment transport over gobi could be predicted by an Owen-type saltation model: $q = A\rho/g u_*(u_*^2 - u_{*_t}^2)$, where q is sediment transport rate, A is a soil-related dimensionless factor, u_* is the friction velocity, u_{*_t} is the threshold friction velocity, g is the gravitational acceleration, ρ is the air density. This study indicates that the sediment flux sampling using horizontal and vertical sediment traps coupled to weighing sensors provides a practical method to determine values for A in this model that can provide good estimates of sediment transport rates in gobi areas.

1. Introduction

Gobi, a rough surface, usually comprises a single surface layer of coarse clasts in various sizes from gravel to boulder underlain by fine silts and sands with very few coarse particles (Cooke and Warren, 1973). Gobi is actually a regional name of desert pavement in Asia from Mongolian, and it is widely distributed in northwest China with an area of 661,000 km^2 (State Forestry Administration, 2011). This kind of surface is common in deserts, known variously as gibber, reg or hamada in other arid regions of the world (Livingstone and Warren, 1996). Such surfaces are almost ubiquitous on Mars (Lancaster et al., 2010). Gobi is usually smooth, stable and with less sand deposition and thus often becomes the main location of engineering construction and transportation lines. However, gobi is mainly located in strong wind areas, it is a major source area of dust storms in northern China, and the damage caused by intense sediment flux is serious (Zhang et al., 2014). In recent years, the exploitation of the gobi surface has increased in China, and a large area of solar and wind energy power station has already been built on it. At present, with the operation of the second Lanzhou–Xinjiang railway as well as the idea of "new silk road economic belt" being implemented, the speed of the regional economic development in northwest China even in Central Asia will be further accelerated, while the exploitation of the gobi surface will inevitably cause more wind-blown sand problems.

Aeolian sediment transport is one of the important geomorphic processes operating in arid regions, which involves strong interaction between the wind and the ground surface (Nickling and Neuman, 2009). It creates various problems, such as obscuring the sun, impeding traffic, damaging crops and electrical switches, abrading paint, has a negative impact on human health and can cause degradation of valuable and nonrenewable soil resources (Fryrear and Saleh, 1993). Aeolian sediment transport over rough surfaces like gobi is different from that over smooth surfaces because of the presence of non-erodible roughness elements such as gravels or cobbles. These roughness elements can absorb a proportion of wind shear stress, and thus the total wind shear stress acting on these surfaces can be divided into two parts: the shear stress acting on non-erodible roughness elements and that on the intervening surfaces between them (Schlichting, 1936). Addi-

* Corresponding author at: No. 320, Donggangxi Road, Lanzhou 730000, Gansu, China. Tel.: +86 931 4967541; fax: +86 931 8277169.

http://dx.doi.org/10.1016/j.aeolia.2016.03.002
1875-9637/

tionally, they exert an impact to the grain–bed interaction. Although significant advances have been made in our understanding of aeolian transport process in the past few decades, the effect of surface roughness, especially solid roughness elements, on it is still uncertain (Lancaster et al., 2010). Moreover, aeolian sediment transport over these rough surfaces have been mainly investigated by wind tunnel experiments (e.g., Al-Awadhi and Willetts (1999), Dong et al. (2004), Gillette and Stockton (1989), Lyles et al. (1974), McKenna Neuman (1998), Mckenna Neuman and Nickling (1995) and Tan et al. (2013)), yet relatively few studies have focused on it in a field view (e.g., Gillies and Lancaster (2013) and Gillies et al. (2006)). Wind tunnel results cannot be fully applied to the comparison with those in field situations in relation to scale issues (Gillies et al., 2006), and thus field studies with extensive instrumentation are required.

In this paper, we report on field observation results of aeolian sediment transport over a rough surface-gobi atop the Mogao Grottoes, China, during dust storms using vertical and horizontal sediment traps coupled to two weighing sensors. Special attention was paid to the effect of surface roughness on sediment entrainment and saltation mass flux and to establishment of the relationship between friction velocity and sediment transport rate for the gobi surface. This research will provide theoretical reference for sand drift control on the gobi surface, and it is also an attempt to realistically predict sediment transport rates for complex surface types on Earth.

2. Study site

The Mogao Grottoes, a buddhist shrine, are located about 25 km southeast of Dunhuang City and are known as the "world's art gallery" or "the museum on a wall", which were built on the south-north-oriented steep cliff (1680 m long and 10–45 m high) incised by a river. Gobi and mega-dunes are two main landforms on the top surface of the Mogao Grottoes. Mingsha Mountain, a huge and complex mega-dune, is located to the west side atop the grottoes, which is the main sand source threatening the burial of grottoes. The study site is situated in the central part of the gobi surface atop the Mogao Grottoes at latitude 40.05°N, longitude 94.80°E (Fig. 1). The gobi surface, where observations of aeolian sediment transport were performed, mainly consists of gravels in size ranging from 30 to 50 mm and in the coverage of 30–40%, which is underlain mainly by fine sand (mean grain size, 210 μm). Wind regimes show there are three prevailing winds atop the Mogao Grottoes: easterly, westerly and southerly winds, of which easterly and westerly winds are two main strong winds that transport sediments dominating in April of each year (Liu et al., 2011; Zhang et al., 2014). Thus, the measured transport events in this study were concentrated in dust storms generated from easterly or westerly winds.

3. Materials and methods

Instantaneous sediment transport over gobi was measured by a newly-developed vertically-integrated passive sediment trap, which can weigh the total collected sediment automatically by a weighing sensor connected to a data logger (Fig. 2). This sediment trap, with a total height of 0.5 m, width of 150 mm and thickness of 75 mm, is composed of a bottom rectangular steel box (300 × 300 × 200 mm), 16 rectangular aluminum sampling orifices and 16 cloth bags for collecting sediments. The bottom 10 orifices are 75 mm wide and 24 mm high and the upper 6 orifices are 75 mm wide and 42 mm high. The back of each orifice was connected to a cloth bag that could be removed after a run to weigh the collected sediments inside. The three bottom cloth bags were not fixed at the ends of the orifices but in the bottom box in order to prevent them to overlap each other as collecting sediments and thus to increase the sampling efficiency; the other 13 bags were fixed at the ends of the orifices. The weighing sensor has an area of 300 × 300 mm and the measurement range is 0–25 kg with a precision of 1 g (Fig. 2). The acquisition frequency ranges from 0.1 to 3600 s and in this study, it was set as 60 s. This transport measurement system has been proved to be effective in the research of aeolian processes through a recent portable wind tunnel study (Zhang et al., 2014).

Wind speed profiles were measured with five-cup anemometers at the respective heights of 0.2, 0.5, 1.0, 1.5 and 2.0 m, and wind direction was measured with a wind vane set at a height of 2 m, which were all recorded every 60 s by a data logger because of the limitation of the anemometer resolution. Wind speed, wind direction and sediment transport were measured synchronously on time.

The entrainment threshold friction velocity was measured using a horizontal sediment trap, which contains a cylindrical steel drum with both a diameter and height of 0.4 m coupled to a weighing sensor using the same data logger with the weighing sensor under the vertical sediment trap. The steel drum was laid under the gobi surface and on the weighing sensor, and it was set flush

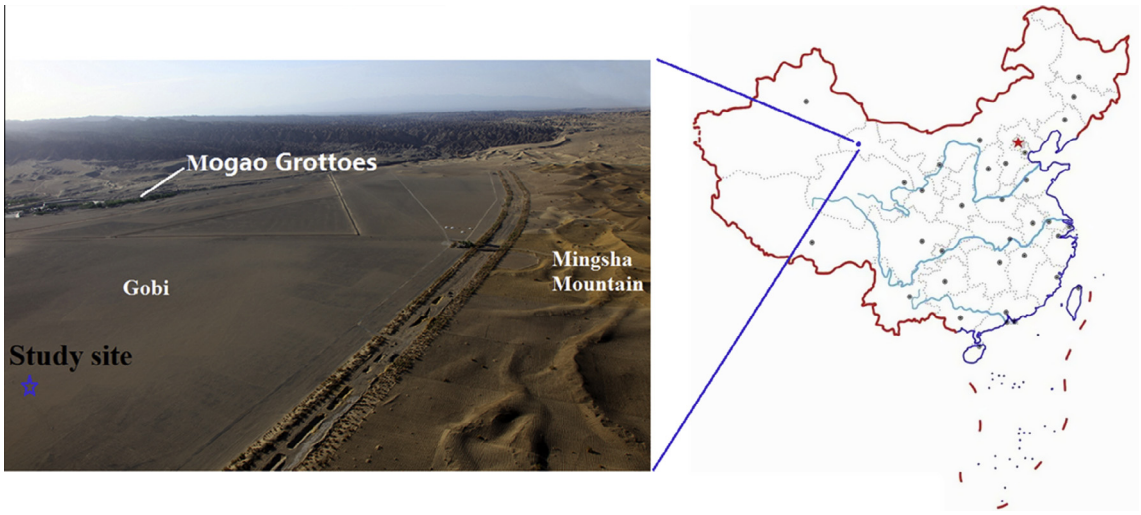

Fig. 1. The location of the study site. The aerial view looking south of the study site.

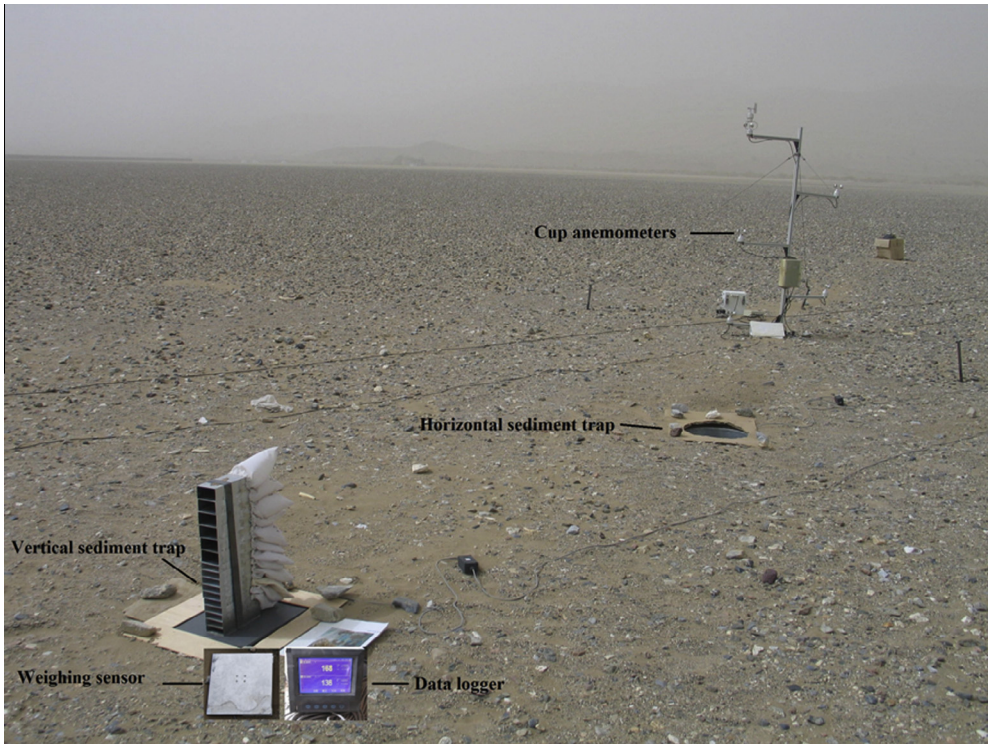

Fig. 2. Synchronized measurement of sediment entrainment, saltation mass flux and wind speeds on the studied gobi surface.

with the gobi surface. The surrounding gap between the gobi surface and the horizontal sediment trap was covered by a board with a circular hole of the same size to the steel drum's diameter (Fig. 2).

4. Results and discussion

4.1. Sediment transport events

Four sediment transport events were observed during the field work from 5, April 2013 to 30, April 2013, of which one was generated by W winds and three by NNE winds. Table 1 shows the summarized characteristics of the four measured sediment transport events. The measurement duration fell in between 150 and 660 min. The average wind speed at a height of 2 m ranged from 7.14 to 9.76 m s^{-1}; the respective mean wind friction velocity was in the range of 0.36–0.55 m s^{-1}. During the first two transport events, one sampling run was conducted in the measurement duration and five runs mostly ranging in length from 90 to 160 min for the last two transport events. Mean rates of sediment transport ranged from 1.36 to 7.62 g m^{-1} s^{-1}.

4.2. Sediment flux density profile

In periods of sediment transport events, sediment flux density decreased exponentially with increasing height (Fig. 3), which differed significantly from results of wind tunnel experiments that the flux density profile over gobi presented a non-monotone curve (e.g., Dong et al. (2004) and Qu et al. (2005)). At the same study site, our recent portable wind tunnel results revealed that in most cases sand flux density decreased exponentially with height only above 50–80 mm, while they increased with increasing height below this critical height (Tan et al., 2013), and thus the profile also showed a non-monotone curve shape as the above mentioned wind tunnel results.

4.3. Threshold wind friction velocity

In the single transport event of April 15, 2013, when measurement began, wind speed had already been larger than the threshold, and thus the quantity of trapped sediments in the horizontal sediment trap increased with measurement continuing. As wind decreased below the threshold, the accumulated sediment quantity no longer increased, thus reaching a maximum value of 3.8 kg (Fig. 4a). In terms of the variation rate of accumulated sediment quantity, the value was zero below the threshold velocity, and as over the threshold, the variation rate increased apparently, indicating sediment entrainment occurred. The corresponding threshold wind speed at a height of 2 m was 5.7 m s^{-1} (Fig. 4b). Threshold wind friction velocity (u_{*_t}) was estimated using the wind profile data as sediment initiated according to the method reported by Bauer et al. (1992) and Wiggs et al. (1996). The calculated u_{*_t}

Table 1
Characteristic parameters of the measured transport events.

Date	Measurement duration (min)	Max wind speed at 2 m	Mean value			
			Wind direction (°)	Wind speed at 2 m (m s^{-1})	Friction wind speed (m s^{-1})	Sediment transport rate (g m^{-1} s^{-1})
20130408	150	10.7	11.3	8.16	0.43	1.36
20130415	200	11.3	256.4	7.14	0.36	2.00
20130417	660	15.3	26.0	9.76	0.55	7.62
20130428	510	14.2	29.3	9.43	0.55	7.14

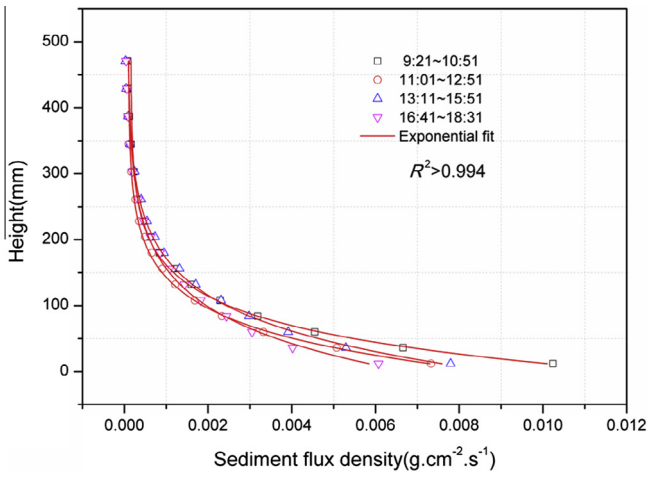

Fig. 3. Sediment flux density profiles over gobi atop the Mogao Grottoes (runs 1–4 in transport event-20130417 for example).

value during the westerly wind in transport event-20130415 was 0.28 m s^{-1}. Similarly, during the transport event of April 8, 2013, in the commencement of measurement, sediments also had already been entrained; during the measurement period, the total accumulated sediment quantity reached 5.9 kg (Fig. 4c). When wind speed decreased below the threshold, the total quantity of trapped sediments no longer varied with continuing measurement. The threshold wind speed at a height of 2 m was 6.1 m s^{-1}, and as wind speed was greater than this value, the variation rate of accumulated sediment quantity increased noticeably (Fig. 4d). The calculated u_{*_t} value in the transport event of NNE wind was 0.33 m s^{-1}.

4.4. Grain size distribution of sediment flux

Grain size parameters were determined using the geometric method of moments in the GRADISTAT software (Blott and Pye, 2001). For the two single events of April 15, 2013 and April 17, 2013, sediments transported within the height of 282 mm were fine in grade (mean grain size, 0.125–0.15 mm), and then they became very fine in grade above 282 mm (mean grain size, 0.07–0.12 mm) (Fig. 5). The pattern of particle size changing as a function of height during these two events showed an increase in mean grain size within 216 mm and 240 mm, respectively, while the mean grain size decreased conspicuously with height above these two critical height values.

Sorting values increased with increasing height within the layer of 0–409 mm, and they ranged from moderately well and moderately sorted to poorly sorted according to the categorization of Blott and Pye (2001). However, this trend reversed at a height of 409 mm above the gobi surface and sorting values began to decrease with height, but they were also poorly sorted (Fig. 5).

The skewness in the trap samples at different heights was dominated by fine skewed distribution (0–324 mm, 75% of all samples). The pattern of skewness changing as a function of height was sim-

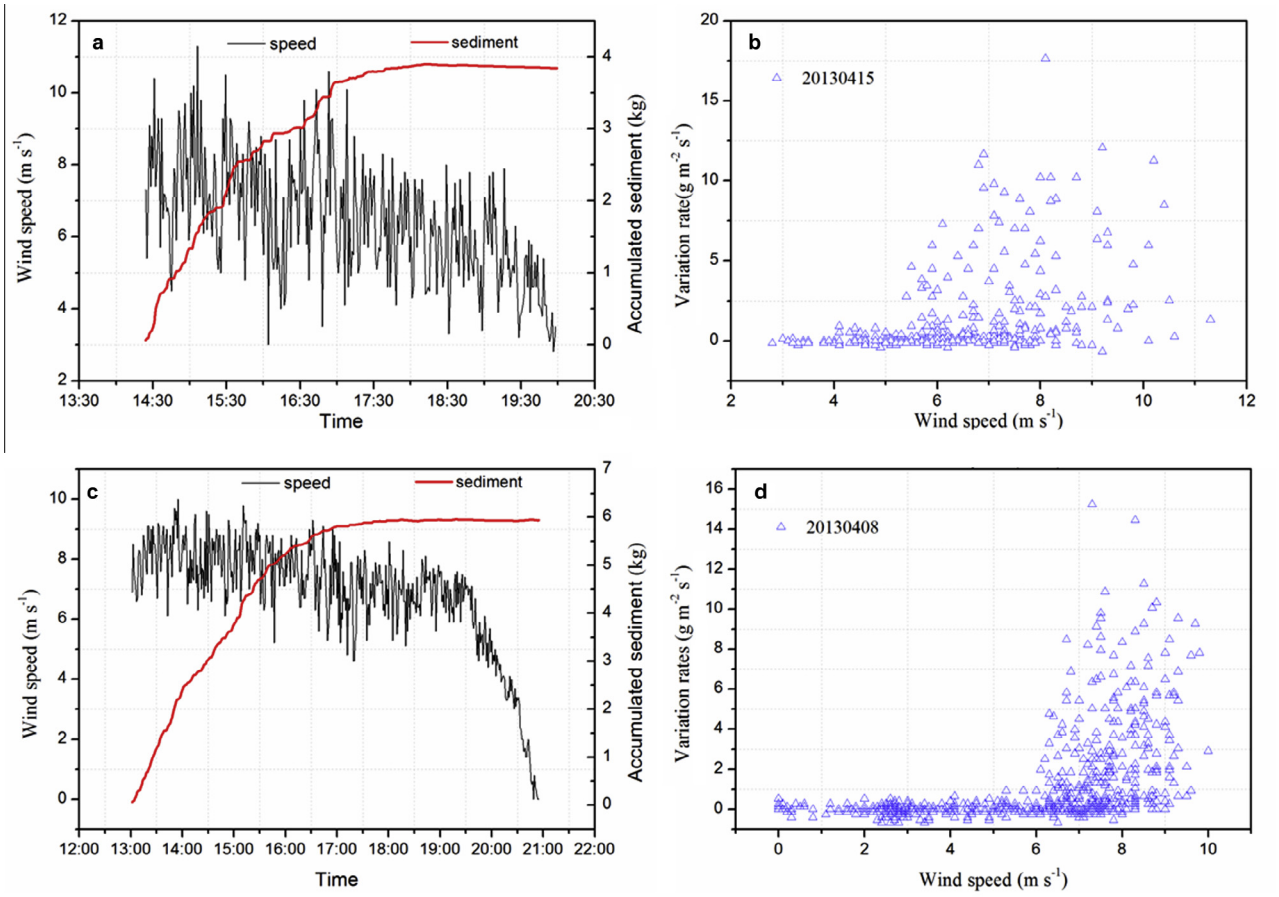

Fig. 4. The relationship between wind speed at a height of 2 m and the weight of accumulated sediment in the horizontal sediment trap during transport events of 20130415 (a) and 20130408(c); Variation rates of the accumulated sediment in horizontal sediment trap in unit area and time changing with wind speed at a height of during transport events of 20130415(b) and 20130408(d).

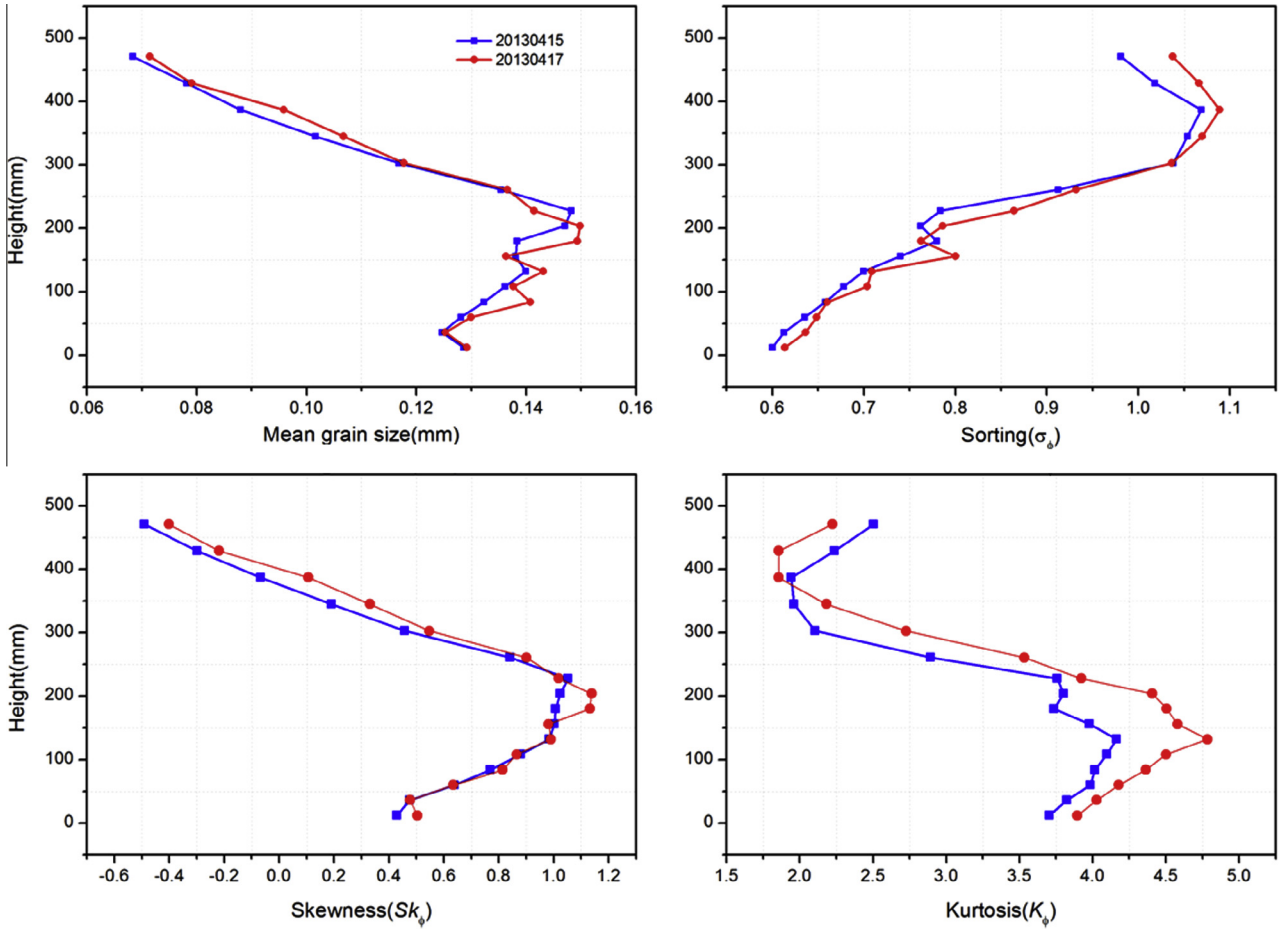

Fig. 5. Mean grain size, sorting, skewness and kurtosis changing with height during transport events of 20130415 and 20130417.

ilar to that of the mean grain size. The kurtosis was dominated by the leptokurtic form (68.75% of all samples) (Fig. 5).

4.5. Prediction of sediment transport rate

In prediction of aeolian transport, sediment transport rates are generally proportional to the cube of wind speed or wind friction velocity like those models of Bagnold (1941) and Kawamura (1951), in which steady winds and dry sand surface are assumed.

In this study, each run of sediment transport measurement last over several hours, and thus major wind direction change could contribute to the variations of sediment transport rate. In order to increase the efficiency of sediment trap impacted by wind direction variation, data of sediment transport rate in each run of the transport event of April 17, 2013 was selected only in duration when wind direction change was small (Fig. 6). Results showed that aeolian sediment transport over gobi followed a similar Owen (1964) saltation equation (Fig. 7):

$$q = A\rho/g u_*(u_*^2 - u_{*_t}^2) \quad (1)$$

where q is the average sediment transport rate in 5 min, u_* is the corresponding average friction velocity, u_{*_t} is the threshold friction velocity, g is the gravitational acceleration, ρ is the air density, A is a soil-related dimensionless parameter (Gillette and Ono, 2008). The mean transport rate used here represented the shortest time fraction that produced strong correlation with the wind record. This modified Owen saltation equation was also called the Gillette model (Ono, 2006).

For equally strong winds and the same soil, the parameter A is constant (Gillette and Ono, 2008). Thus, the value of A determined from the transport data of April 17 and wind data of April 28 (u_*) can be applied to the prediction of sediment transport rates during the latter transport event. Similarly, data of the measured sediment transport rates on April 28 was also selected only in the duration with small wind direction variations. Results reveal that the predicted transport rates q_p were consistent with the measured values q_m and the R^2 value reached 0.856 (Fig. 8). This also indicated that during events of sediment transport over gobi, the relationship between transport rate and wind friction velocity could be expressed by the Owen-type saltation equation.

5. Discussion

5.1. Sediment flux density profile

As described earlier, the sediment flux density profile over gobi followed an exponential form, which is apparently different from previous wind tunnel results that sediment flux density varied with height in a non-monotone curve. Zhang et al. (2011) demonstrated that the curve shape of sediment flux over gobi beds was mainly affected by sediments available for transport and that the non-monotone profile mainly occurred in a sediment supply-limited condition while the monotone one usually in an unlimited sediment supply condition. According to the field observation results, the parameter A of the studied gobi surface was 0.551, while the average value was 0.10 for all runs in our portable wind tunnel experiments (Tan et al., 2013). Meanwhile, the soil-related

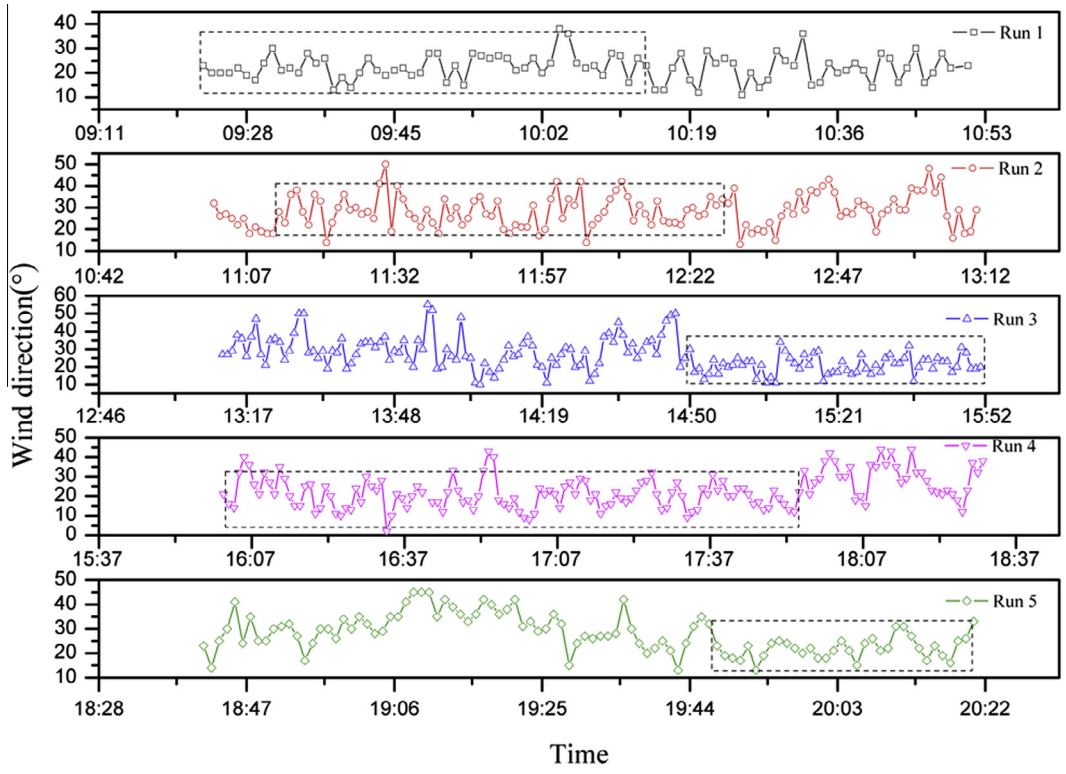

Fig. 6. Wind direction variation in each run during the transport event of April 17th, 2013. Duration in the dotted box was selected to do analysis on the prediction of sediment transport rates.

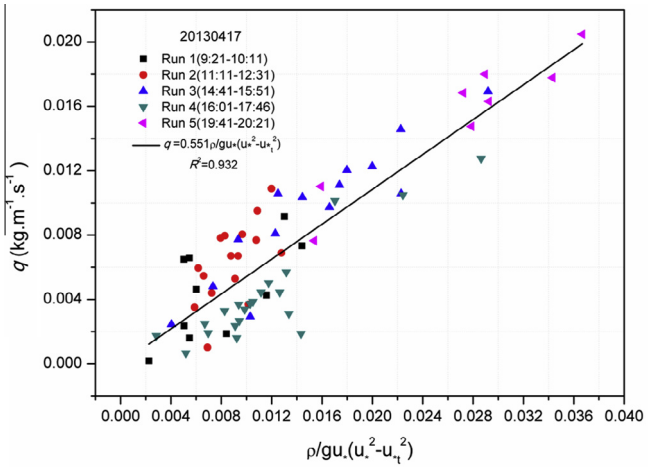

Fig. 7. Sediment transport rates q over gobi in a time scale of minute during dust storm on April 17th, 2013 changing with $\rho/gu_*(u_*^2 - u_{*_t}^2)$ in Eq. (1). Duration in each run was in accordance with that in the dotted box in Fig. 6.

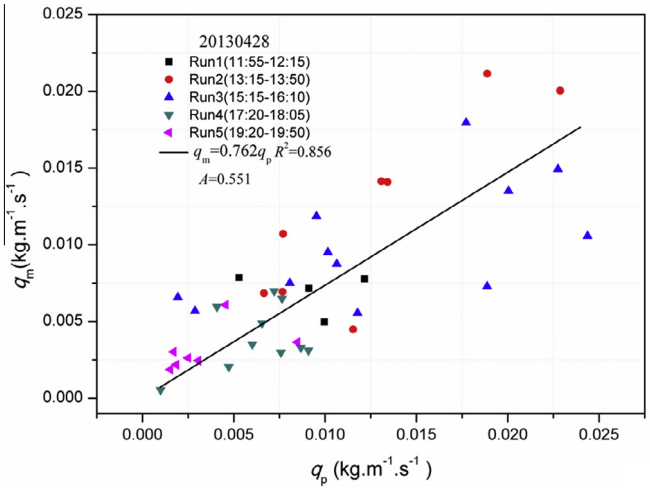

Fig. 8. Comparison between the predicted sediment transport rate q_p calculated using wind speed data of dust storm on April 28th, 2013 and the measured transport rate q_m on April 28th, 2013.

parameter A in Eq. (1) can be used to express the possibility of sand supply limitation (Gillette and Ono, 2008). Thus, the sediments available for transport in the field were clearly more sufficient than that in the wind tunnel. In this case, it was understandable that sediment flux density profiles over gobi were in a monotone curve shape and those in the portable wind tunnel were non-monotone.

In addition, the difference in the measured curve shape of sediment flux density profile over gobi in wind tunnel experiments and field observation may attribute to the scale difference of the boundary layer. The boundary layer in the portable wind tunnel is in a scale of 100 mm. The height of gravels on the studied gobi surface approximately ranges from 10 mm to 30 mm, and these gravels occupy about 10–30% of the wind tunnel boundary layer in height. Thus, the effect of gravels on the boundary layer adjustment is significant in the wind tunnel: the velocity profiles over the rough surfaces exhibit a substantial reduction in shear near the surface, which is called the roughness sublayer, whose height exceeds the height of roughness elements by a factor of 2 and 5 (McKenna Neuman, 1998; Raupach, 1991). Accordingly, this can result in the decrease of sediment flux density in the height range of 20–150 mm, which is in general agreement with the height of the peak flux exhibiting in previous wind tunnel results. However, in the field the boundary layer can reach several hundred meters,

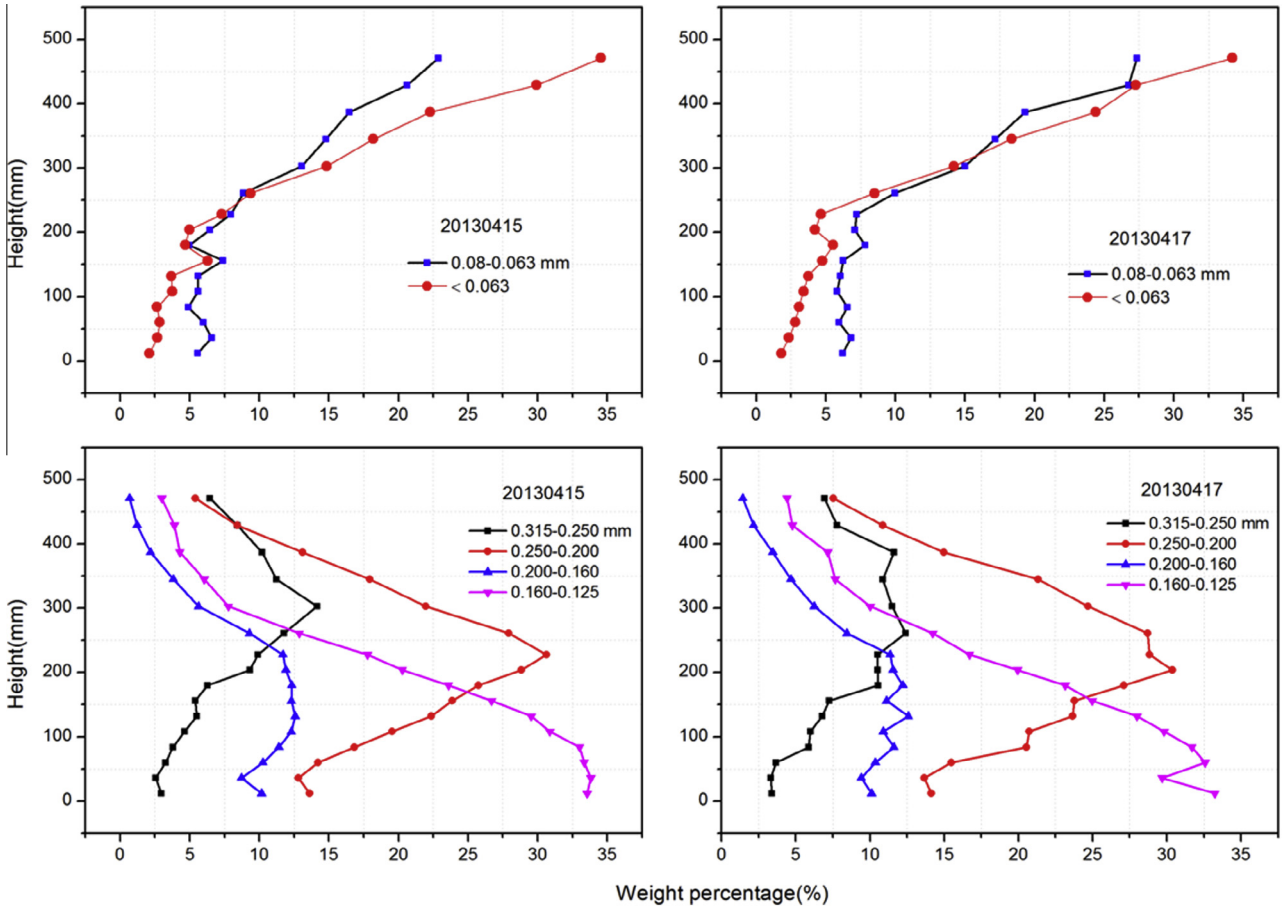

Fig. 9. Weight percentages of relative fine grains (<0.08 mm) (a) and coarse grains (0.125–0.315 mm) (b) changing as a function of height.

and thus gravels only occupy approximately one in ten thousand of the height of the boundary layer. Consequently, the impact of gravels on sediment flux density profile over gobi is not so remarkable in the field scale as that in the wind tunnel. Furthermore, it should be noted that the improvement of measurement techniques for the flux profile such as sediment traps with high-resolution, especially in the near-surface layer, will be of continuing significance as reported by Dong et al. (2006), in which wind tunnel results revealed that the peak flux did exist at a height even above a loose sand surface (1–24 mm) based on the measurement of particle velocity and concentration by particle image velocimetry.

5.2. Threshold wind friction velocity

The presence of non-erodible gravels increased the threshold friction velocity for sediment entrainment, which was mainly via the local partitioning of shear stress in gravels. As shown earlier, the measured u_{*_t} of the studied gobi surface was 0.28–0.33 m s^{-1}, and the corresponding threshold wind speed at a height of 2 m was between 5.7 and 6.1 m s^{-1}. Comparatively, the calculated u_{*_t} using the method reported by Bagnold (1941) was 0.15–0.19 m s^{-1} for 125–160 μm. Thus, the non-erodible roughness elements-gravels on gobi surface increased the threshold friction velocity for sediment entrainment by approximately 1.8 times compared to a uniform sand surface. Lancaster et al. (2010) and Raupach et al. (1993) also demonstrated that the non-erodible roughness elements increase the threshold velocity for sediment transport. In low wind friction velocities, gravels act as traps for wind-blown sand, and the increase in threshold friction velocity for sediment entrainment will eventually attenuate sediment transport and thus aeolian transport hazards. The trapping effect of gravels has been used to control sand drift disasters threatening the grottoes in the study area (Li et al., 2014; Zhang et al., 2014).

5.3. Grain size distribution of sediment flux

In this study, there is a coarsening trend in the profile of mean grain size with height within the layer of 0–216 mm or 0–240 mm differing in wind directions, and then the infection points occurred and mean grain size began to decrease. This result was completely different from that the mean grain size of sediment flux over sand surfaces decreased monotonously (Arens et al., 2002), increased (Van der Wal, 2000) or first decreased then increased with height (Farrell et al., 2012; Tan et al., 2014; Williams, 1964). Theoretically, it is generally believed that grain size decreases with height above the bed surface, while the coarsening trend of mean grain-size with height requires that the coarser grains have higher launch velocities than finer grains. The mechanism for the coarsen trend in the mean grain size as a function of height is still unclear (Farrell et al., 2012). The clear decrease in mean grain size above 240 mm seems to be connected with the increase of coarser grains (0.125–0.315 mm) in mass weight while the decrease of finer grains (<0.08 mm) in this layer (Fig. 9). Essentially, characteristics of the grain size distribution of sediment flux over gobi may be attributed to the difference in the distribution of lift-off velocities and angles between coarse and fine grains plus their complex collision with gravels.

5.4. Prediction of sediment transport rate

As showed earlier, our field measurement results showed the saltation mass flux over gobi behaved like an Owen-type saltation

equation, which clearly differs from those models of Bagnold (1941) and Kawamura (1951), and in these models, sediment transport rates are generally proportional to the cube of wind speed (u) or the wind friction velocity (u_*). This result also corroborates wind tunnel results of Gillette and Stockton (1989) that the relationship between sediment transport rate and wind friction velocity followed an Owen function for erodible surfaces covered by non-erodible roughness elements. Recently, our portable wind tunnel experiments on aeolian transport over gobi with different gravel coverages showed that above the threshold velocity, sediment flux over gobi also behaved like an Owen-type saltation equation in accordance with Eq. (1) (Tan et al., 2013). Thus, this study indicates that the observation method of aeolian transport using horizontal and vertical sediment traps coupled to weighing sensors can effectively build the relationship between sediment transport rate and wind friction velocity, and results of these field studies can also be applied to the corresponding revalidation of wind tunnel experiment results.

6. Conclusion

Gobi is a natural rough surface on Earth. Field studies on aeolian sediment transport over a gobi surface atop the Mogao Grottoes using horizontal and vertical sediment traps coupled to weighing sensors have provided a useful data set on the entrainment of sediment particles between gravels and transport over the rough surface by wind. The effect of non-erodible roughness elements-gravels clearly increase the entrainment threshold compared with the sand surface without non-erodible roughness elements mainly because of the absorption of wind momentum by gravels.

The exponential form of the flux profile measured on the gobi surface indicates that the effect of gravels on sediment flux density profile is not so apparent in a field scale as that in wind tunnels, where the saltation mass flux shows a non-monotone curve shape in most cases. Both the observed transport data of two dust storms with measurement duration of 8.5–11 h and our recent portable wind tunnel experiments demonstrate that aeolian sediment transport over gobi surface can be predicted by a similar Owen saltation equation or Gillette Model as described by Ono (2006). This model can be applied to the prediction of sediment transport rate based on the local wind friction velocity, the entrainment threshold, and the soil-related parameter A of a given gobi surface.

Acknowledgements

This work was supported by the STS-HHS Plan Project of Cold and Arid Regions Environmental and Engineering Research Institute, CAS, China, the National Science Foundation of China (41271023, 41401408, 41371102) and the National Science & Technology Pillar Program (2013BAK01B01, 2013BAC07B00). We thank Mr. Guobin Zhang, Fei Qiu, Hongtao Zhan, Rui Li and Shuanghu Lin for their assistance in the field work.

References

Al-Awadhi, J.M., Willetts, B.B., 1999. Sand transport and deposition within arrays of non-erodible cylindrical elements. Earth Surf. Processes Landforms 24, 423–435.
Arens, S.M., van Boxel, J.H., Abuodha, J.O.Z., 2002. Changes in grain size of sand in transport over a foredune. Earth Surf. Processes Landforms 27, 1163–1175.
Bagnold, R.A., 1941. The Physics of Windblown Sand and Desert Dunes. Methuen, London, p. 265.
Bauer, B.O., Sherman, D.J., Wolcott, J.F., 1992. Sources of uncertainty in shear stress and roughness length estimates derived from velocity profiles. Prof. Geogr. 44, 453–464.
Blott, S.J., Pye, K., 2001. GRADISTAT: a grain size distribution and statistics package for the analysis of unconsolidated sediments. Earth Surf. Processes Landforms 26, 1237–1248.
Cooke, R.U., Warren, A., 1973. Geomorphology in Deserts. Batsford, London.
Dong, Z., Qian, G., Luo, W., Wang, H., 2006. Analysis of the mass flux profiles of an aeolian saltating cloud. J. Geophys. Res.: Atmos. 111 (D16) (1984–2012).
Dong, Z., Wang, H., Liu, X., Wang, X., 2004. A wind tunnel investigation of the influences of fetch length on the flux profile of a sand cloud blowing over a gravel surface. Earth Surf. Processes Landforms 29, 1613–1626.
Farrell, E., Sherman, D., Ellis, J.T., Li, B., 2012. Vertical distribution of grain size for windblown sand. Aeolian Res. 7, 51–61.
Fryrear, O.W., Saleh, A., 1993. Field wind erosion: vertical distribution. Soil Sci. 155, 294–300.
Gillette, D.A., Ono, D., 2008. Expressing sand supply limitation using a modified Owen saltation equation. Earth Surf. Processes Landforms 33, 1806–1813.
Gillette, D.A., Stockton, P.H., 1989. The effect of nonerodible particles on wind erosion of erodible surfaces. J. Geophys. Res.: Atmos. 94, 12885–12893 (1984–2012).
Gillies, J.A., Lancaster, N., 2013. Large roughness element effects on sand transport, Oceano Dunes, California. Earth Surf. Processes Landforms 38 (8), 785–792.
Gillies, J.A., Nickling, W.G., King, J., 2006. Aeolian sediment transport through large patches of roughness in the atmospheric inertial sublayer. J. Geophys. Res.: Earth Surf. 2003–2012, 111.
Kawamura, R., 1951. Study on Sand Movement by Wind. Reports of the Institute of Science & Technology University of Tokyo, University of Tokyo, vol. 5, pp. 95–112.
Lancaster, N., Nickling, W.G., Gillies, J.A., 2010. Sand transport by wind on complex surfaces: field studies in the McMurdo Dry Valleys, Antarctica. J. Geophys. Res. 115, F03027.
Li, G.S., Qu, J.J., Li, X.Z., Wang, W.F., 2014. The sand-deposition impact of artificial gravel beds on the protection of the Mogao Grottoes. Sci. Rep. 4 (10), 4341.
Liu, B., Zhang, W., Qu, J., Zhang, K., Han, Q., 2011. Controlling windblown sand problems by an artificial gravel surface: a case study over the gobi surface of the Mogao Grottoes. Geomorphology 134, 461–469.
Livingstone, I., Warren, A., 1996. Aeolian geomorphology: an introduction. Longman.
Lyles, L., Schrandt, R.L., Schmeidler, N.F., 1974. How aerodynamic roughness elements control sand movement. Trans. ASAE 17, 134–139.
McKenna Neuman, C., 1998. Particle transport and adjustments of the boundary layer over rough surfaces with an unrestricted, upwind supply of sediment. Geomorphology 25, 1–17.
Mckenna Neuman, C., Nickling, W.G., 1995. Aeolian sediment flux decay: non-linear behaviour on developing deflation lag surfaces. Earth Surf. Processes Landforms 20, 423–435.
Nickling, W.G., Neuman, C.M., 2009. Aeolian sediment transport, Geomorphology of Desert Environments. Springer, pp. 517–555.
Ono, D., 2006. Application of the Gillette model for windblown dust at Owens Lake, CA. Atmos. Environ. 40, 3011–3021.
Owen, P.R., 1964. Saltation of uniform grains in air. J. Fluid Mech. 20, 225–242.
Qu, J.J., Huang, N., Tuo, W.Q., Lei, J.Q., Dong, Z.B., 2005. Structural characteristics of gobi sand-drift and its significance. Adv. Earth Sci. 20, 19–23.
Raupach, M., Gillette, D., Leys, J., 1993. The effect of roughness elements on wind erosion threshold. J. Geophys. Res.: Atmos. 98 (D2), 3023–3029 (1984–2012).
Raupach, M.R., 1991. Saltation layers, vegetation canopies and roughness lengths. Acta Mech. (Suppl 1), 83–96.
Schlichting, H., 1936. Experimentelle untersuchungen zum rauhigkeitsproblem. Arch. Appl. Mech. 7, 1–34.
State Forestry Administration, 2011. A Bulletin of Status Quo of Desertification and Sandification in China. China's State Forestry Administration, pp. 1-20.
Tan, L., Zhang, W., Qu, J., Du, J., Yin, D., An, Z., 2014. Variation with height of aeolian mass flux density and grain size distribution over natural surface covered with coarse grains: a mobile wind tunnel study. Aeolian Res. 15, 345–352.
Tan, L., Zhang, W., Qu, J., Zhang, K., An, Z., Wang, X., 2013. Aeolian sand transport over gobi with different gravel coverages under limited sand supply: a mobile wind tunnel investigation. Aeolian Res. 11, 67–74.
Van der Wal, D., 2000. Grain-size-selective aeolian sand transport on a nourished beach. J. Coastal Res., 896–908
Wiggs, G.F., Livingstone, I., Warren, A., 1996. The role of streamline curvature in sand dune dynamics: evidence from field and wind tunnel measurements. Geomorphology 17, 29–46.
Williams, G., 1964. Some aspects of the eolian saltation load. Sedimentology 3, 257–287.
Zhang, W., Tan, L., Zhang, G., Qiu, F., Zhan, H., 2014. Aeolian processes over gravel beds: field wind tunnel simulation and its application atop the Mogao Grottoes, China. Aeolian Res. 15, 335–344.
Zhang, W., Wang, T., Wang, W., Liu, B., 2011. Wind tunnel experiments on vertical distribution of wind-blown sand flux and change of the quantity of sand erosion and deposition above gravel beds under different sand supplies. Environ. Earth Sci. 64, 1031–1038.